

Electronic Supplementary Information (ESI) for:

Two-dimensional Tellurium nanosheets for photoacoustic imaging-guided photodynamic therapy

Yan Lin,^a Ying Wu,^a Rong Wang,^b Tao Guo,^a Pei-Fu Luo,^a Xiang Lin,^a Juan Li,^a Guoming Huang^{*b} and Huang-Hao Yang^{*a}

^aMOE Key Laboratory for Analytical Science of Food Safety and Biology, Fujian Provincial Key Laboratory of Analysis and Detection Technology for Food Safety, State Key Laboratory of Photocatalysis on Energy and Environment, College of Chemistry, Fuzhou University, Fuzhou 350116, P. R. China.

^bCollege of Biological Science and Engineering, Fuzhou University, Fuzhou 350116, P. R. China

*Correspondence authors: G. Huang (gmhuang@fzu.edu.cn.) and H. H Yang (hhyang@fzu.edu.cn)

Experimental section

Materials. Te powder, N, N-Dimethylformamide (DMF), Glutathione (GSH), Dichlorofluorescein diacetate (DCFH-DA), 1,3-Diphenylisobenzofuran (DPBF) were purchased from Sigma-Aldrich. 2,2,6,6-tetramethylpiperidine (TEMP) was purchased from J&K Scientific Ltd (Beijing, China). Calcein-AM and propidium iodide (PI) were purchased from Beyotime Biotechnology (Beijing, China). Ultrapure water was obtained from a Milli-Q water purification system (18.2 M Ω resistivity, Millipore).

Apparatus. Transmission electron microscopy (TEM) and high-resolution TEM (HRTEM) were performed on a Tecnai G2 F20 at an accelerating voltage of 200 kV. Electron spin resonance (ESR) was performed on a JES-FA200 (JEOL, Japan) spectrometer with X-band microwave frequency of 9.4 GHz at room temperature. The Fourier transform infrared (FTIR) spectrum was collected on a Thermo fisher Nicolet 6700. The tellurium concentration of the samples was determined by a XSERIES 2 ICP-MS. Multispectral optoacoustic tomography was carried out on the InVision 128 MSOT system (iThera Medical, Germany). Tauc plots were collected on a UV-vis Spectrophotometers (Thermo Scientific Evolution 200 Series) and the data were processed by Kubelka–Munk method. X-ray photoelectron (XPS) and valence band XPS (VB-XPS) spectra were obtained by a Thermo escalab 250Xi XPS spectrometer. X-ray diffraction (XRD) pattern was collected by using an X-ray powder diffractometer (D/MAX-3C, Rigaku Co., Japan). The fluorescence images of cells were taken on a confocal laser scanning microscope (CLSM) (Nikon A1, Japan) and inverted fluorescence microscope (Nikon Ti-S, Japan). Atomic force microscope (AFM) measurement was performed on a Multimode 8 microscope (Bruker, USA).

Synthesis of Te nanosheets@GSH. The Te nanosheets were synthesized by liquid exfoliation of the corresponding Te raw powder. Briefly, 60 mg of Te powders were first dispersed in 100 mL of DMF. Then, the mixture solution was sonicated in water for 8 h. Afterward, the solution was centrifuged at 5000 rpm for 10 min to remove the unexfoliated particles, and then the supernatant was centrifuged at 10000 rpm for 10 min to collect the Te nanosheets. Finally, the obtained Te nanosheets were mixed with

10 mM GSH by sonication and then the mixture was stirred overnight. The excess GSH was removed by centrifugation at 10000 rpm for 10 min, and the precipitate products were collected.

Detection of reactive oxygen species (ROS). DPBF was used for ROS detection. In detail, 200 μL of Te nanosheets@GSH aqueous solution (0.4 mM of Te, determined by ICP-MS) was added into 1.8 mL of DPBF (80 μM), and the mixture was stirred in dark for 2 h. A LED light (670 nm) was employed as the light source. The sample was measured by UV-vis at different times. The NaN_3 was served as the scavenger for ROS, and the added concentration was 40 $\mu\text{g mL}^{-1}$.

Cytotoxicity assay. The cytotoxicity was measured using a standard MTT assay. HeLa cells were cultured in RPMI-1640 medium with 10% fetal bovine serum at 37 °C in a humidified atmosphere with 5% CO_2 . HeLa cells were seeded in 96-well plates and then incubated with 100 μL of Te nanosheets@GSH with different Te concentrations. After the incubation for 24 h, the culture medium was replaced by 100 μL of a new MTT (0.5 mg mL^{-1}) mixed culture medium and the plate was incubated for 4 h at 37 °C. The supernatant was removed, and each well was added with 200 μL of dimethyl sulfoxide (DMSO). The OD_{490} value (Abs.) of each well was collected by an SH-1000 Lab microplate reader subsequently. Cell viability was determined from the OD_{490} value of the experimental group by subtracting that of the blank group.

Intracellular ROS detection. HeLa cells were first incubated with 0.1 mM of Te nanosheets@GSH at 37 °C for 12 h in 96-well plates. Then, 10 mM DCFH-DA was added into the cells medium and incubated for 30 min. Subsequently, the 96-well plates were illuminated by the LED light (670 nm) for 10 min. Finally, the well plates were imaged by a Nikon A1 confocal laser scanning microscope.

In Vitro MSOT. Different concentrations of Te nanosheets@GSH solutions (0, 5, 10, 15, 20, 25 $\mu\text{g mL}^{-1}$) were filled into agar gel cylinders. The optoacoustic signals were collected by scanning from 680-980 nm (5 nm wavelength for each slice). After the reconstruction for 680 nm, the MSOT images were obtained. Photoacoustic intensity values were measured by finely analyzing regions of interest (ROIs) of the corresponding images.

***In Vivo* MSOT.** MSOT scanning was first performed before the injection of Te nanosheets@GSH, which used as controls. Next, the mice were intratumorally or intravenously injected with Te nanosheets@GSH (100 μ L, 20 μ g mL⁻¹). After that, the mice were scanned from 680 nm to 980 nm to collect signals (5 nm wavelengths for each slice, the region of interest is 25 mm). The body temperature of the mouse was maintained at \sim 37 $^{\circ}$ C during the experiment by using a water heating system.

***In Vitro* photodynamic therapy.** First, Hela cells were incubated with Te nanosheets@GSH at 37 $^{\circ}$ C for 4 h. After that, the cell viability was evaluated using a standard MTT assay. To image the cell viability, the cells were co-stained with Calcein AM and propidium iodide (PI), and then were imaged by a Nikon Eclipse Ti-S inverted microscope.

***In Vivo* photodynamic therapy.** Animal experiments were executed in accordance with the Guide for the Care and Use of Laboratory Animals (Ministry of Science and Technology of China, 2006) and were approved by Institutional Animal Care and Use Committee of Fuzhou University. The tumor mode was prepared by subcutaneously injecting a suspension of 2×10^6 HepG2 cells in PBS (100 μ L) into the back of the hind leg of BALB/c nude mice (weight \sim 25 g). For *in vivo* tumor therapy, the mice were divided into four group (five mice per group): (i) blank group (ii) Te nanosheets@GSH only group, (iii) light only group, (iv) Te nanosheets@GSH + light group. For group (i) and group (iii) the mice were received an intratumoral injection of 100 μ L saline, and then the group (iii) was irradiated with a 670 nm light (160 mW cm⁻²) for 10 min. For group (ii) and (iv), Te nanosheets@GSH (100 μ L, 20 μ g mL⁻¹) was intratumorally injected to the mice, after that the group (iv) was further irradiated with a 670 nm light (160 mW cm⁻²) for 10 min. The tumor volume was calculated according to the equation: tumor volume = (length \times width²)/2. Relative tumor volumes were calculated as V/V_0 where V is the tumor volume calculated after the treatments, while V_0 is the initial tumor volume before the treatments.

Biodistribution analysis. To investigate the tissue biodistribution, Te nanosheets@GSH were intravenously injected into the mice (100 μ L, 20 μ g mL⁻¹). Then the mice were sacrificed at different time points (6 h, 12 h, 24 h, and 48 h post-

injection), and major organs including heart, liver, spleen, lung, kidney, and tumor were extracted. These tissues were treated with HNO₃-H₂O₂ digestion, and Te concentration in these samples was determined by ICP-MS.

Histology. Sixteen days later the injection of saline or Te nanosheets@GSH, the mice were sacrificed and the main tissues (heart, liver, spleen, lung, kidney and tumor) were excised for preparing histological sections. The histological sections then were stained with hematoxylin and eosin (H&E) following the standard protocol.

Supporting Figures

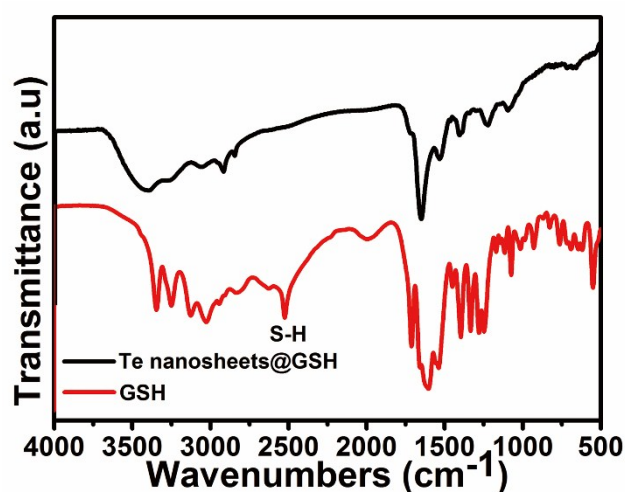


Fig. S1. The Fourier transform infrared (FTIR) spectrum of the GSH and GSH modified Te nanosheets (Te nanosheets@GSH).

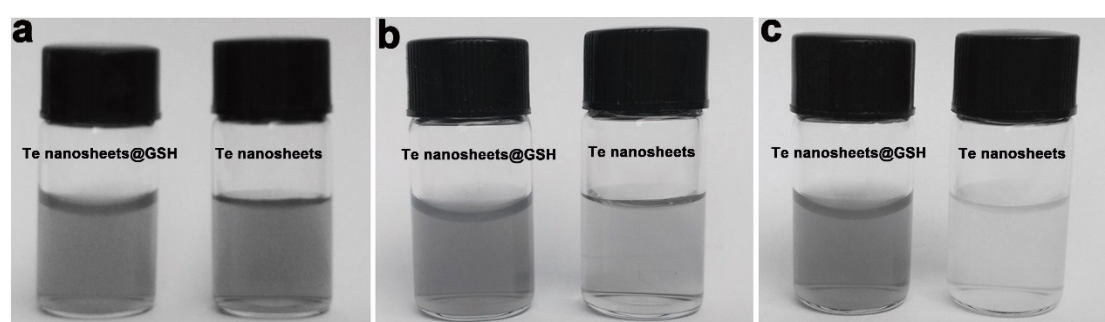


Fig. S2. Digital photographs of Te nanosheets and Te nanosheets@GSH aqueous solution collected at (a) 0 day, (b) 3 days, (c) and 7 days.

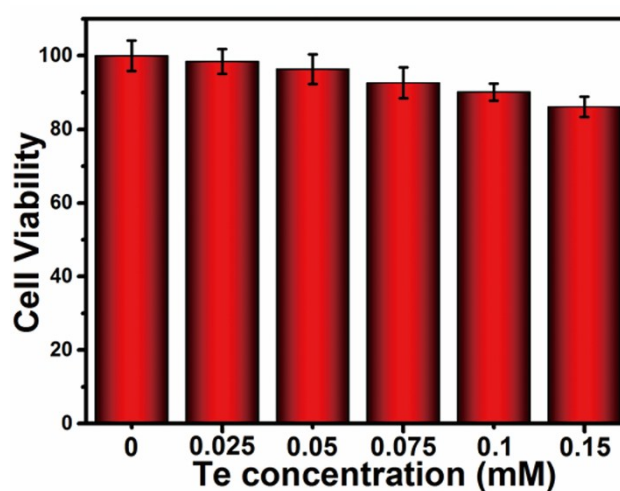


Fig. S3. Cell viability of HeLa cells after incubated with Te nanosheets@GSH with different concentrations.

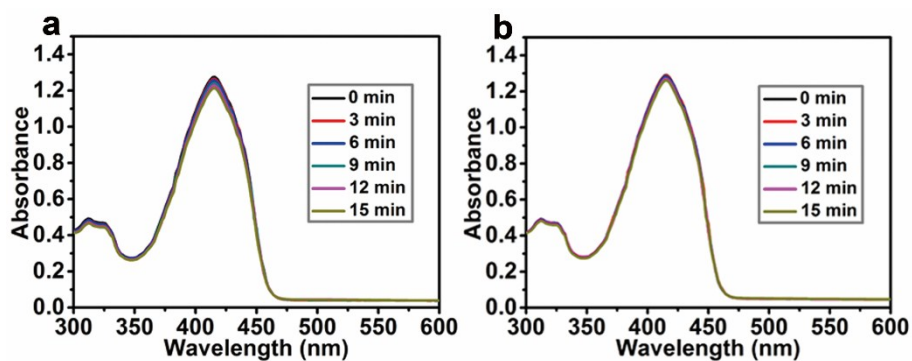


Fig. S4. Absorption spectra of DPBF at different irradiation time points under different conditions: (a) in the presence of Te nanosheets@GSH + NaN_3 , (b) in blank control.

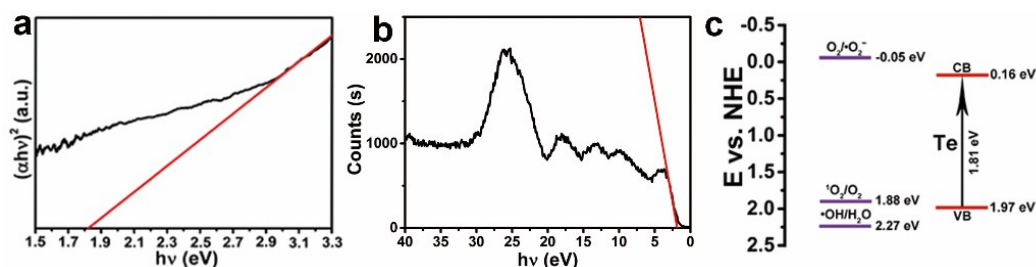


Fig. S5. (a) Tauc plots of Te nanosheets@GSH for calculating the band gap energy (E_g). (b) VB-XPS of Te nanosheets@GSH for calculating energy level of VB (E_{VB}). (c) Band energy levels of Te nanosheets@GSH and reduction potentials of $\text{O}_2/\bullet\text{O}_2^-$, $^1\text{O}_2/\text{O}_2$, and $\bullet\text{OH}/\text{H}_2\text{O}$.

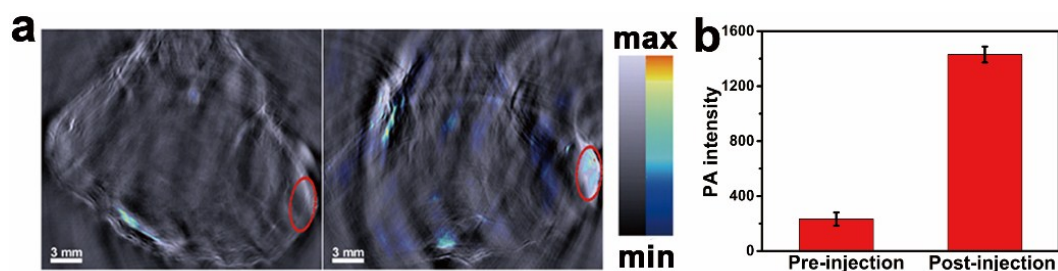


Fig. S6. (a) *In vivo* MSOT images and (b) corresponding quantification of intensities of mice in tumor region pre- and post-intravenous injection of Te nanosheets@GSH ($100 \mu\text{L}$, $20 \mu\text{g mL}^{-1}$), respectively.

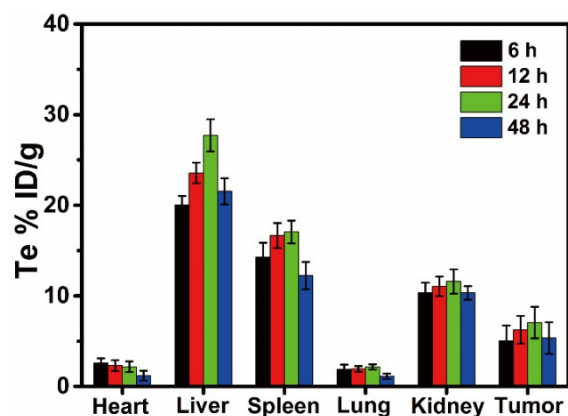


Fig. S7. Biodistribution of Te nanosheets@GSH in major organs after the intravenous administration ($n = 3$).

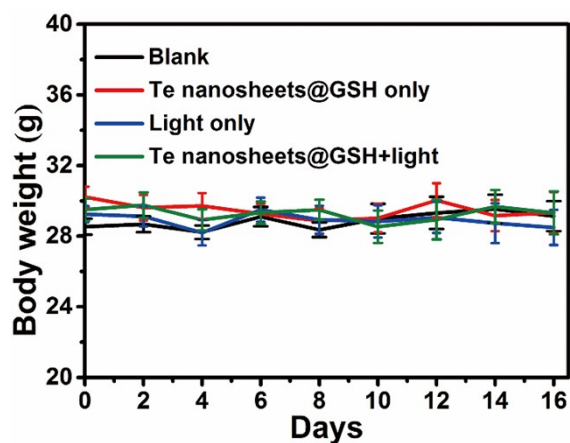


Fig. S8. Body weight changes of the HepG2 tumor-bearing mice after different treatments.

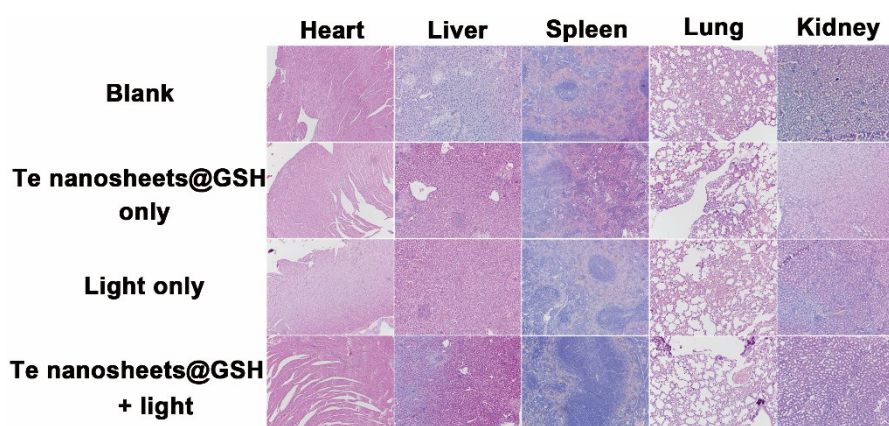


Fig. S9. H&E stained images of major organs of mice 16 days after different treatments.